JOURNAL OF AIRCRAFT
Vol. 43, No. 2, March–April 2006

Engineering Notes

ENGINEERING NOTES are short manuscripts describing new developments or important results of a preliminary nature. These Notes should not exceed 2500 words (where a figure or table counts as 200 words). Following informal review by the Editors, they may be published within a few months of the date of receipt. Style requirements are the same as for regular contributions (see inside back cover).

Flexible- and Rigid-Wing Micro Air Vehicle: Lift and Drag Comparison

Anthony M. DeLuca* and Mark F. Reeder†
U.S. Air Force Institute of Technology, Wright–Patterson Air Force Base, Ohio 45433-7542
Jacob Freeman‡
U.S. Air Force Research Laboratory, Eglin Air Force Base, Florida
and
Michael V. Ol§
U.S. Air Force Research Laboratory, Wright–Patterson Air Force Base, Ohio 45433-7542

Nomenclature

b	=	wing span
C_D	=	drag coefficient
C_L	=	lift coefficient
$C_{L\alpha}$	=	lift curve slope
c	=	wing root chord
c_{bar}	=	wing mean chord
q_∞	=	freestream dynamic pressure, $\frac{1}{2}\rho U_\infty^2$
Re_c	=	Reynolds number based on wing root chord
U_∞	=	tunnel freestream velocity, ft/s
α	=	angle of attack relative to the bottom of the vehicle fuselage
α_{L0}	=	Angle of Zero Lift
α_{stall}	=	angle of wing stall

Introduction

MINIATURIZATION of unmanned air vehicles in military applications leading toward the so-called micro air vehicles (MAV) has introduced considerable challenges in aerodynamic efficiency, handling and control. The U.S. Air Force Research Laboratory, Munitions Directorate, Flight Vehicles Integration Branch developed a MAV with a flexible wing for U.S. Air Force Special Tactics Teams. The flexible wings can be folded, allowing storage of the MAV in a compact tube.

Although the flexible wing design is motivated by packaging reasons, the wing flexibility itself may provide a benefit as a passive flow control device, mitigating stall and improving gust tolerance, which would be a crucial performance improvement for low-inertia, low-maneuverability fixed-wing MAVs.[1] For the typical fixed-wing MAV Reynolds numbers on the order of 10^5, separation of the laminar boundary layer just aft of the leading-edge suction peak results in a detached shear layer that often does not transition soon enough to reattach over the airfoil surface, resulting in stall at small angles of attack.[2] The primary goal of this investigation was to characterize how the flexibility of the wing affects performance for a specific MAV, with the expectation that at moderate angles of attack the wing flexure could affect separation bubble formation and at higher angles of attack would delay stall.

Experimental Setup

The flexible wing, based on a model developed at the University of Florida,[3] has a carbon-fiber leading edge extending to approximately $x/c = 0.25$. Carbon-fiber ribs extending toward the trailing edge support a parachute-latex membrane forming the remainder of the wing. This design allows the wings to be folded beneath the fuselage.

A series of tests was performed in the U.S. Air Force Institute of Technology low-speed wind tunnel (closed test section, 9.5:1 contraction ratio, and test section 31 by 44 by 72 in. (see Ref. 3), details given in Ref. 4) to determine the effect of wing flexure on aerodynamic loads. To isolate the effects of wing flexibility, a second MAV with a rigid carbon-fiber wing of the same shape was also tested. The two vehicles are shown in Fig. 1. Both aircraft (Fig. 1) had 24-in. span and 6-in. root chord. Table 1 summarizes the geometry of each aircraft. The only control surfaces are ruddervators on a V-tail with approximately 107 deg included angle. This Note only covers zero-sideslip, propeller-removed, clean-empennage data; results for control surface deflection, power-on effects, and sideslip effects are given by Deluca.[4]

The force and moment data were collected with an Able Corporation MKII nominal 8-lbf, six-component internal strain gauge balance (accurate to 0.25% of full capacity) secured in a block mounted under the fuselage bottom. The block closely matched that of a camera pod on the vehicle, and identical blocks were produced for each model. Test conditions are summarized in Table 2.

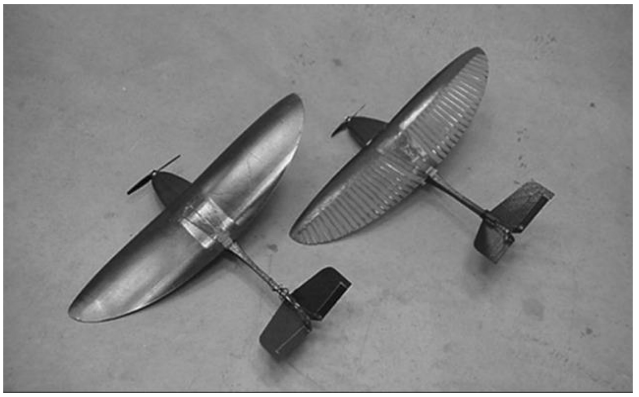

Fig. 1 Rigid-wing and flexible-wing MAVs.

Presented as Paper 2004-2396 at the AIAA 24th Aerodynamic Measurement Technology and Ground Test Conference, Portland, OR, 1–28 July 2004; received 19 January 2005; revision received 23 August 2005; accepted for publication 26 August 2005.

*Graduate Student, Department of Aeronautics and Astronautics. Member AIAA.
†Assistant Professor, Department of Aeronautics and Astronautics. Member AIAA.
‡Advanced Munitions Research Engineer, Munitions Directorate. Member AIAA.
§Aerospace Engineer, Air Vehicles Directorate. Senior Member AIAA.

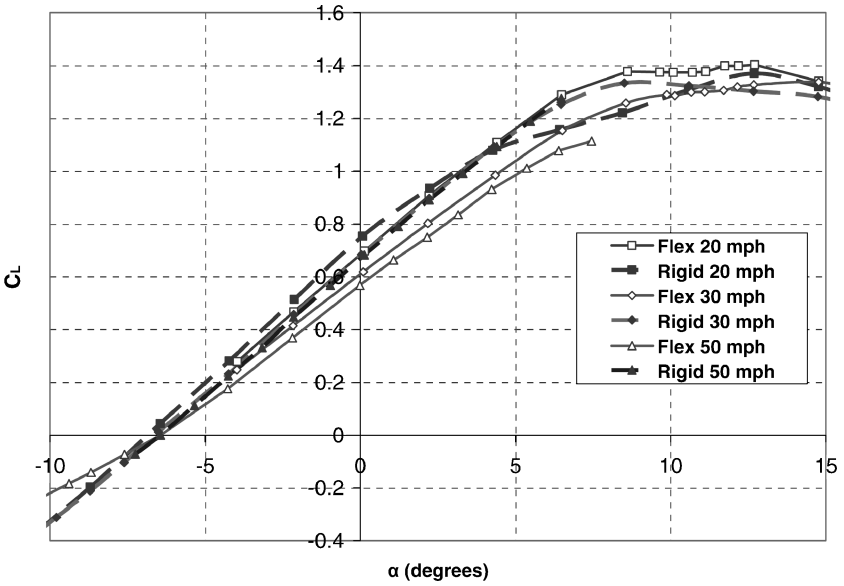

Fig. 2 Comparison of lift coefficient vs angle of attack for flexible and rigid wings.

Table 1 MAV geometric properties

Property	Value
Wing planform area	93.5 in.^{2}
Root chord c	6″
Mass, flexible-wing vehicle	0.705 lbm,
Mass, rigid-wing vehicle	0.794 lbm
Mean aerodynamic chord c_{bar}	4.2 in.
Span b	24 in.
Wing leading-edge thickness	0.025 in.
Parachute planform thickness (for the flexible wing)	0.005 in.
Aspect Ratio	6.16

Table 2 Summary of test conditions

U_∞, mph	q_∞, psf	Re_c
20	0.90	8.55×10^4
30	2.16	1.32×10^5
50	6.15	2.23×10^5

The reference value for $\alpha = 0$ deg corresponds to the flat bottom of the fuselage level with the freestream.

The measurements that influence the accuracy of the results given here include U_∞, ambient pressure, ambient temperature, α, and the load measurements, axial force and normal force. An error analysis[4] showed that, of these, the two most prominent contributors to uncertainty in the measurements were that of airspeed and axial force. The full span of the axial force gauge was 5 lbf, with manufacturer specified resolution of 0.0125 lbf. Balance drift was monitored during testing, and it was well below the minimum resolution. The most restrictive condition for the axial balance gauge was the minimum drag point for the lowest speed runs, 20 mph. Under this condition, the measured axial force was found to be 0.04 lbf. Effects due to blockage and upwash due to image vortices were corrected by standard wind-tunnel methods.[5] Note that values for α are referenced to the flat bottom of the fuselage. Thus, the wing angle of attack was positive when at the referenced $\alpha = 0$ deg setting.

Results

Wind-tunnel data for C_L and C_D vs α are given in Figs. 1 and 2, respectively. The 50-mph runs were limited to $\alpha \leq 7$ deg due to balance load limit constraints. In all cases, α_{L0} was found to be approximately -6.5 deg, and stall was found to proceed gradually with increasing α. For the rigid wing, the values of the C_L and the linear portion of the lift curve are comparable for each airspeed tested. However, the flexible wing shows a slight reduction in the lift slope for larger dynamic pressures. This is consistent with a flexure of the aft portion of the wing in response to aerodynamic loading. If Reynolds number effects were dominant, one might have anticipated a mild increase in the lift slope as dynamic pressure increases. Thus, it is reasonable to conclude that, in this Reynolds number range, the aeroelastic deformation effects dominate for this flexible-wing aircraft.

The lift curve for the rigid wing rolls off for $\alpha \geq 4$ deg for the 20-mph case, whereas for the 30- and 50-mph cases this drop was not exhibited until $\alpha \geq 6$ deg. This is consistent with the general trends of increasing Reynolds number over a wing. By contrast, the 20-mph flexible-wing lift slope remains mostly linear until $\alpha \geq 6$ deg, suggesting that stall is mitigated by flexibility.

Figure 3 shows that, throughout the range of angles of attack, the flexible wing was found to have a slightly lower drag than the rigid-wing aircraft, with the difference increasing with increasing angle of attack.

Drag values for the two wings converge toward each other as the stall angle is approached. There was no evidence of a reverse drag bucket at moderate angles of attack, which suggests that the separation bubble does not grow from short to long, or burst to form an open separation at any angle of attack below stall.

A commercial code (FLUENT) was utilized to perform the computational fluid dynamics (CFD) analysis. Computations were run with a steady, incompressible, second-order upwind scheme with a segregated, implicit solver and a mesh size of approximately 10^6 cells. Results typically converged by 1500 iterations. Aeroelastic effects were not modeled; therefore, the simulation is a representation of the rigid wing. Computations were run both laminar and with a k–ε turbulence model. Lift and drag data from both the laminar and turbulent results at 30 mph are in Fig. 4. The turbulent cases only covered $\alpha \geq 6$ deg. The experimental lift slope is slightly steeper and the measured drag coefficient was slightly higher than their respective CFD predictions for each case. The turbulent computations show slightly higher maximum C_L, though the stall behavior is similar to the laminar case.

Figure 5a shows experimentally measured L/D vs α for both the flexible and rigid wings at 20, 30, and 50 mph, whereas Fig. 5b shows a comparison of the computational and experimental data at 30 mph, with error bars on the latter. The flexible-wing MAV exhibited a higher maximum L/D and maintained a broader range of α where L/D remained above 6. For the rigid wing, the L/D peak broadened with increasing velocity, but there was no clear increase

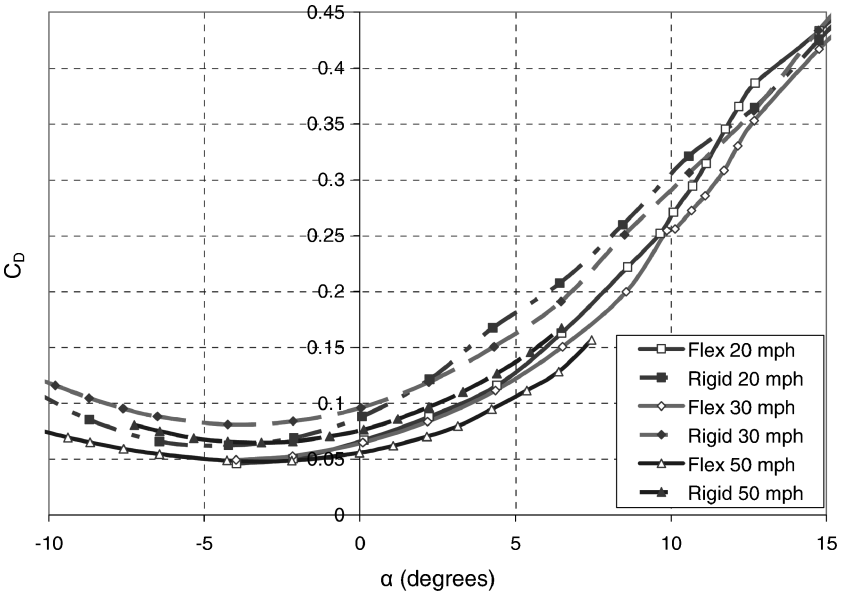

Fig. 3 Comparison of drag coefficient vs angle of attack for flexible and rigid wings.

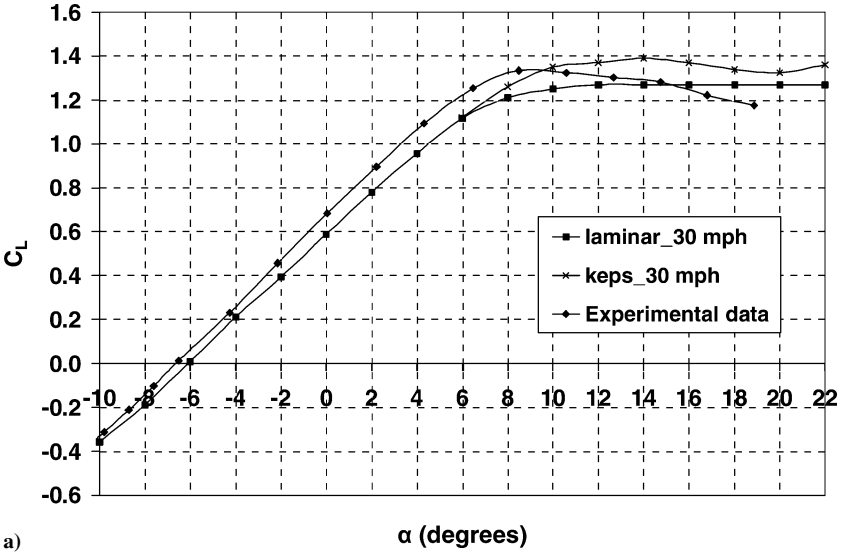

a)

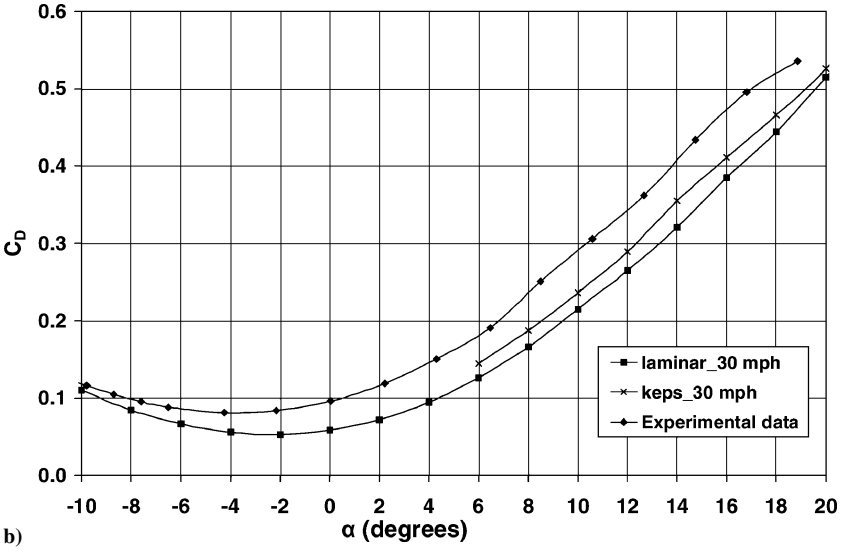

b)

Fig. 4 CFD vs experiment, rigid-wing MAV: a) C_L vs α and b) C_D vs α.

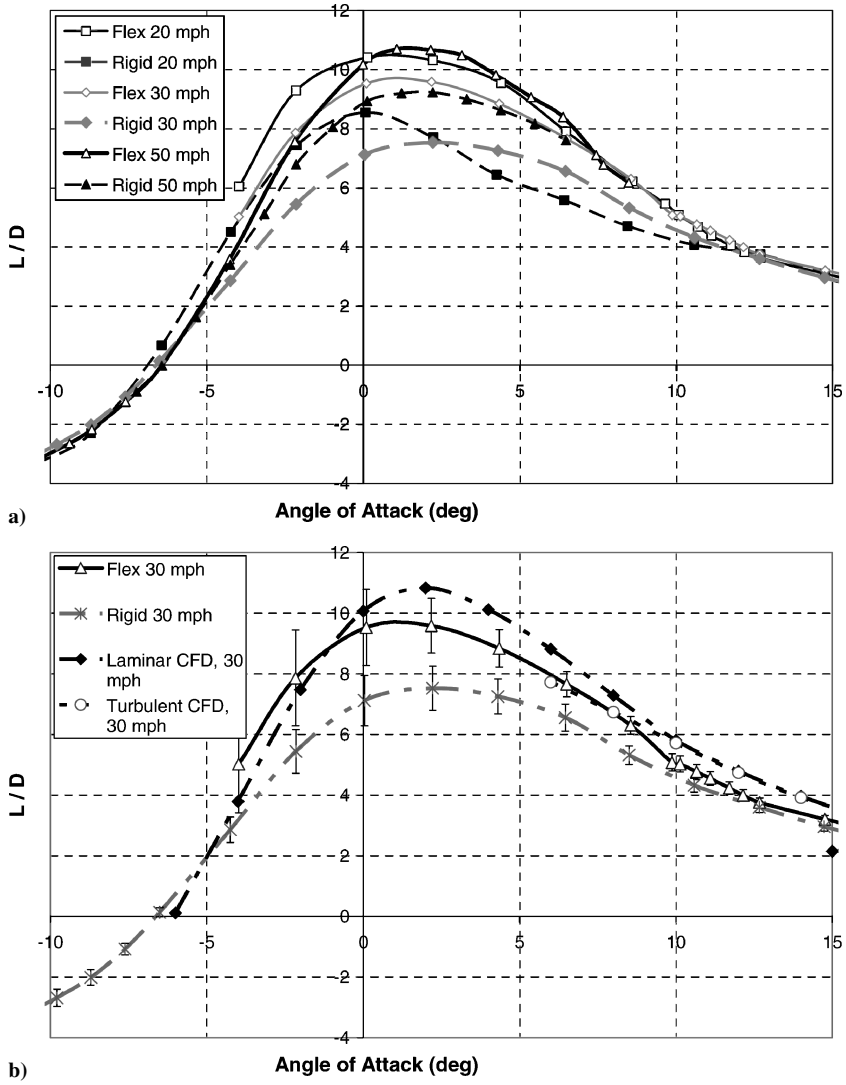

Fig. 5 ***L/D*** **for flexible and rigid wing for a) all speeds, experimental data only and b) 30-mph case comparing experiment and computation.**

of its peak value with increasing velocity. For the flexible wing, the point of maximum L/D shifts toward higher angles (in the region of $0 < \alpha < 4$ deg). For the 20- and 30-mph data, which is close to the vehicle's typical operating speed, the flexible-wing MAV had an $L/D_{\max} \approx 10$, whereas the rigid-wing MAV had an $L/D_{\max} \approx 8$.

Conclusions

Wind-tunnel testing at flight-representative speeds for a fixed-wing MAV with a flexible wing and with a geometrically identical rigid wing showed a higher L/D ratio for the latter, at airspeeds ranging from 20 to 50 mph. The range of angles of attach for its peak L/D was also found to be broader than that of the rigid-wing vehicle. For the higher airspeeds, the flexible wing's lift curve slope decreased, presumably due to aeroelastic deformation associated with increasing local dynamic pressure, which leads to aerodynamic washout. The flexible wing stalled at higher angle of attack than the rigid wing, particularly for the 20-mph case. This may be attributable to a reduction in the size and the effect of a separation bubble, though direct evidence of the bubble was not obtained in this study.

A baseline computational analysis was conducted for the rigid-wing model, with laminar and fully turbulent cases (the latter with a k–ε model). The computed lift slope slightly underpredicted experimental results at 30 mph. The predicted minimum drag coefficient was slightly below that of the measurement.

Acknowledgments

The authors would like to thank Dwight Gehring and Jay Anderson for their technical expertise, which was instrumental in the execution of these experiments, and to acknowledge the guidance and support of John Anttonen and Ian Bautista of the U.S. Air Force Research Laboratory/Munitions Directorate, Flight Vehicles Integration Branch. The views expressed in this article are those of the authors and do not reflect the official policy or position of the United States Air Force, Department of Defense, or the U.S. Government.

References

[1]Lian, Y., Shyy, W., and Ifju, P., "Membrane Wing Model for Micro Air Vehicles," *AIAA Journal*, Vol. 41, No. 12, 2003, pp. 2492–2494.

[2]Mueller, T. J., and Torres, G. E., "Aerodynamic Characteristics of Low Aspect Ratio Wings at Low Reynolds Numbers," *Progress in Astronautics and Aeronautics*, AIAA, Reston, VA, Vol. 195, 2001, Chap. 7, pp. 115–141.

[3]Ifju, P. G., Jenkins, D. A., Ettinger, S., Lian, Y., and Shyy, W., "Flexible-Wing-Based Micro Air Vehicles," AIAA Paper 2002-0705, Jan. 2002.

[4]Deluca, A., "Experimental Investigation into the Aerodynamic Performance of Both Rigid and Flexible Wing Structured Micro-Air-Vehicles," M.S. Thesis, Dept. of Aeronautics and Astronautics, U.S. Air Force Inst. of Technology, Wright–Patterson AFB, OH, 2004.

[5]Barlow, J. B., Rae, W. H., and Pope, A., *Low-Speed Wind Tunnel Testing*, 3rd ed., Wiley, New York, 1999, Chaps. 7–10.